Available online at www.sciencedirect.com
SCIENCE DIRECT
Polymer 47 (2006) 999–1010
polymer
www.elsevier.com/locate/polymer

# Probing the reaction kinetics of vinyl acetate free radical polymerization via living free radical polymerization (MADIX)

Alexander Theis, Thomas P. Davis, Martina H. Stenzel, Christopher Barner-Kowollik*

*School of Chemical Engineering and Industrial Chemistry, Centre for Advanced Macromolecular Design, The University of New South Wales, Sydney, NSW 2052, Australia*

Received 13 October 2005; received in revised form 13 December 2005; accepted 14 December 2005

**Abstract**

Living free radical polymerization technology (macromolecular design via the interchange of xanthates (MADIX)) was applied to give accesses to chain length and conversion dependent termination rate coefficients of vinyl acetate (VAc) at 80 °C using the MADIX agent 2-ethoxythiocarbonylsulfanyl-propionic acid methyl ester (EPAME). The kinetic data were verified and probed by simulations using the PREDICI® modelling package. The reversible addition-fragmentation transfer (RAFT) chain length dependent termination (CLD-T) methodology can be applied using a monomer reaction order of unity, since VAc displays significantly lower monomer reaction orders than those observed in acrylate systems ($\omega$(VAc, 80 °C) = 1.17 ± 0.05). The observed monomer reaction order for VAc is assigned to chain length dependent termination and a low presence of transfer reactions. The $\alpha$ value for the chain length regime of log($i$) = 1.25 − 3.25 (in the often employed expression $k_t(i,i) = k_t^0 i^{-\alpha}$) reads 0.09 ± 0.05 at low monomer to polymer conversion (10%) and increases significantly towards larger conversions ($\alpha$ = 0.55 ± 0.05 at 80%). Concomitantly with a lesser amount of midchain radicals, the chain length dependence of $k_t$ is significantly less pronounced in the VAc system than in the corresponding acrylate systems under identical reaction conditions. The RAFT(MADIX)-CLD-T technique also allows for mapping of $k_t$ as a function of conversion at constant chain lengths. Similar to observations made earlier with methyl acrylate, the decrease of $k_t$ with conversion is more pronounced at increased chain lengths, with a strong decrease in $k_t$ exceeding two logarithmic units from 10 to 80% conversion at chain lengths exceeding 1800.


*Keywords:* Living free radical polymerization (RAFT); Vinyl acetate; Polymerization kinetics and mechanism

## 1. Introduction

Vinyl acetate (VAc) is a highly important monomer and its polymers are used in applications ranging from adhesives, paints, and concrete additives to pharmaceuticals. Since vinyl alcohol itself is not stable and undergoes a rapid rearrangement to acetic aldehyde, poly(vinyl acetate) is an advantageous precursor to poly(vinyl alcohol) (PVAL). PVAL is also interesting within a pharmaceutical context as it is water soluble, non-toxic, non-carcinogenic, easily processed, and displays bioadhesive properties. Furthermore, PVAL can be crosslinked to a hydrogel, i.e. a material able to swell in water and to retain a significant fraction of water within its structure [1]. PVAL gels have been investigated for their suitability for diffuse drug delivery, for oral drug application, and for their bioadhesive nature in drug administration [2,3].

Although VAc is interesting for several applications, there are only limited kinetic data for the VAc polymerization available in literature. The propagation rate coefficient, $k_p$, has been previously investigated by Hutchinson et al. [4,5], and solvent effects of the lumped kinetic parameter $k_p/k_t^{0.5}$ have been studied, too [6,7]. However, to date, no detailed investigations into the termination rate coefficient, $k_t$, of VAc have been performed. Beside the lack of information about the chain length averaged termination rate coefficient, $\langle k_t \rangle$, it would furthermore be very interesting to obtain information about its chain length dependence.

Obtaining reliable data for $k_t$ in free-radical polymerization of different monomers has been an on-going research theme over the last 50 years and to date a variety of methods have been developed to probe this parameter as both a function of the monomer-to-polymer conversion as well as the chain length of the propagating radicals. The complexities involved in obtaining reliable termination rate data as well as a critical

* Corresponding author. Tel.: +61 2 93854331; fax: +61 2 93856250.
*E-mail address:* camd@unsw.edu.au (C. Barner-Kowollik).

0032-3861/$ - see front matter © 2005 Elsevier Ltd. All rights reserved.
doi:10.1016/j.polymer.2005.12.054

evaluation of the most prominent methods for its determination have recently been reviewed [8]. Recent and more advanced methods aim at accessing $k_t(i)$, the termination rate of two macroradicals with equal or similar chain length. Most chain-length dependent (CLD) termination data have been obtained via the detailed analysis of molecular weight data of polymeric material produced by pulsed laser polymerization [9] or by tracing the decay in monomer [10–12] or radical concentration [13,14] after applying a single laser pulse to a polymerizable solution.

A relatively simple but very effective experimental approach to map out the termination rate coefficient as a function of the chain lengths of the terminating radicals by using the reversible addition fragmentation chain transfer (RAFT) polymerization process was recently devised by our group. We termed this approach the RAFT chain length dependent termination technique (RAFT-CLD-T) [15]. Under ideal circumstances, the RAFT methodology [16] allows for a direct correlation of the macromolecular chain length, $i$, with the monomer to polymer conversion. In contrast to many other types of living radical polymerization, which are based on the persistent radical effect, the propagating radical concentration in RAFT mediated polymerizations is—in the case of chain length independent rate coefficients—not affected. Thus, with a relatively simple set of kinetic equations, time dependent rate of polymerization data recorded during a RAFT polymerization (e.g. accessible with a differential scanning calorimetry (DSC) instrument) can be analysed to yield the termination rate coefficient as a function of the chain lengths of the terminating radicals. Previously, we demonstrated that this methodology could be applied to map out chain length dependent termination rate coefficients in styrene [15,17], acrylate [18–20] and methyl methacrylate [21] bulk polymerizations, if the initial RAFT agent is chosen judiciously. Very recently, a variant of the RAFT-CLD-T method was developed in the Göttingen group, using single pulsed laser initiation (SP-PLP RAFT) [20,22], and the RAFT-CLD-T method was extended in our group to map chain length and conversion dependent termination rate coefficients for methyl acrylate [23].

Using the RAFT-CLD-T method, the chain length dependent termination rate coefficient can be calculated via an extended equation, without the need of assuming steady state conditions [18]. The derivation of this equation uses the principle that the change of the radical concentration in a radical polymerization system is given by the difference of radicals generated and radicals terminated at any point in time (Eq. (1)).

$$\frac{\mathrm{d}[P_n]}{\mathrm{d}t} = 2fk_d[I] - 2k_t[P_n]^2 \tag{1}$$

Solving Eq. (1) for $k_t$ leads to Eq. (2).

$$k_t = \frac{2fk_d[I] - (\mathrm{d}[P_n]/\mathrm{d}t)}{2[P_n]^2} \tag{2}$$

The initiator concentration, $[I]$, at any point in time, $t$, can be calculated from the initial initiator concentration and $k_d$, whereas the propagating radical concentration $[P_n]$ can be calculated via the propagation equation using the propagation rate coefficient, $k_p$, and the monomer concentration at time $t$. Thus, Eq. (2) can be rewritten as Eq. (3) [18].

$$\langle k_t \rangle(t) = \frac{2fk_d[I]_0 e^{-k_d t} - \dfrac{\mathrm{d}\left(\dfrac{R_p(t)}{k_p\left([M]_0 - \int_0^t R_p(t)\mathrm{d}t\right)}\right)}{\mathrm{d}t}}{2\left(\dfrac{R_p(t)}{k_p\left([M]_0 - \int_0^t R_p(t)\mathrm{d}t\right)}\right)^2} \tag{3}$$

Since many RAFT agents induce the formation of higher molecular weight polymers already at low monomer to polymer conversions [18,24], the transformation from time dependent $k_t$ to chain length dependent $k_t$ data must be performed using independently determined $M_n$ vs. conversion data (i.e. one can no longer use the theoretically predicted molecular weight evolution). In addition, various initial RAFT agent concentrations need to be employed in order to obtain information in a broad molecular weight range. However, the inherent polydispersity of the polymer samples leads to an averaging of $k_t$ values. Thus—strictly speaking—the reported $k_t(i)$ data are averages of the (very narrow) distribution of chain lengths present at each point in time.

To investigate the termination rate coefficient of VAc via the RAFT-CLD-T method, several aspects need to be considered. Previous reported results show a monomer concentration dependent lumped kinetic parameter $k_p/k_t^{0.5}$ [6], which gives evidence for non-ideal polymerization kinetics of VAc. In other studies carried out by NMR spectroscopy, evidence for chain transfer reactions was found, by H-abstraction from either the backbone or the methyl side-group [25]. To obtain reliable conversion dependent termination rate coefficients, it is necessary to determine the monomer reaction order under conditions close to those used for the RAFT-CLD-T method.

Further, a suitable RAFT agent, which does not cause any rate retardation and provides a leaving group with a similar reactivity as the growing polymer chain must be selected. Since the growing VAc macroradicals are highly reactive, RAFT agents with a low radical stabilization capability must be used in order to allow for a fast fragmentation of the intermediate radicals in the RAFT process.

The low radical stabilization in VAc also causes a slow initiation reaction, when 2,2′-azobisisobutyronitrile (AIBN) is used as initiator [26]. It is thus necessary to analyse whether a slow initiation can affect the outcome of the RAFT-CLD-T method. In the present contribution, we will demonstrate in detail how the RAFT-CLD-T method can successfully be applied to VAc polymerization to obtain reliable results for the chain length dependency of $k_t$ as well as for the determination of its conversion dependency.

## 2. Experimental

### 2.1. Materials

Vinyl acetate (VAc, Aldrich, ≥99%, $M=86$ g mol$^{-1}$) was purified by drying for 1 day over molecular sieve (4 Å) and subsequent distillation in vacuum. 2,2′-Azobisisobutyronitrile (AIBN, DuPont) was recrystallized twice from ethanol before usage. 2-Ethoxythiocarbonylsulfanyl-propionic acid methyl ester was synthesized analogous to literature procedures [41], using methyl 2-bromopropionate instead of methyl bromoacetate and toluene for the subsequent column chromatography.

### 2.2. Polymerizations (DSC)

Solutions of vinyl acetate (VAc) with AIBN and ethyl acetate for the determination of the monomer reaction order, or MADIX agent for the molecular weight and CLD-T measurements were thoroughly deoxygenized via seven subsequent freeze–pump–thaw cycles and handled inside a glove bag filled with dry nitrogen gas. The individual species concentrations can be found in the figure captions describing the associated experiments. Exactly weighed amounts of sample (50–70 mg) were loaded to stainless steel pans that were sealed with an O-ring and stainless steel lids. The polymerization heat was determined isothermally at 80 °C via measuring the heat flow vs. an empty sample pan in a differential scanning calorimeter (Perkin–Elmer DSC 7 with a TAC 7/DX thermal analysis instrument controller). The DSC instrument was calibrated with indium and zinc standards of known mass, melting point temperature and known associated enthalpy change. The rate of polymerization, $R_p$, was calculated using literature values for the heat of polymerization ($\Delta H=-88$ kJ mol$^{-1}$) [27]. For the $M_n$ vs. conversion plots, the sample pans were removed at pre-selected reaction times, corresponding to 5, 10, 25 and 50% conversion and immediately cooled down to 0 °C. The content of each pan was dissolved in THF and subjected to SEC analysis.

### 2.3. Molecular weight analysis

Molecular weight distributions were measured via size exclusion chromatography (SEC) on a Shimadzu modular system, comprising an auto injector, a Polymer Laboratories 5.0 μm bead-size guard column ($50\times7.5$ mm$^2$), followed by three linear PL columns ($10^5$, $10^4$ and $10^3$ Å) and a differential refractive index detector. The eluent was tetrahydrofuran (THF) at 40 °C with a flow rate of 1 mL min$^{-1}$. The system was initially calibrated using narrow polystyrene standards ranging from 540 to $2\times10^6$ g mol$^{-1}$. The resulting molecular weight distributions have been recalibrated using the Mark–Houwink parameters for poly(vinyl acetate) ($K=16.0\times10^{-5}$ dL g$^{-1}$, $a=0.70$) [28]. The Mark–Houwink parameters for polystyrene read ($K=14.1\times10^{-5}$ dL g$^{-1}$ and $a=0.70$) [29].

### 2.4. Densities measurements

The densities of VAc were measured via an Anton Paar DMA 5000 density meter. Since the boiling point of VAc at ambient pressure is at 72 °C, the density at 80 °C was determined by linear extrapolation of the densities determined at 60 °C ($\rho=0.880$ g cm$^{-3}$) and 70 °C ($\rho=0.866$ g cm$^{-3}$). The extrapolated density was found to be $\rho(80\,^\circ\text{C})=0.852$ g cm$^{-3}$.

### 2.5. Simulations

All simulations were carried out using the program package PREDICI®, version 5.36.5, on a Pentium III 800EB, or Athlon XP 2500+ IBM compatible computer.

## 3. Results and discussion

### 3.1. Free radical polymerization kinetics of vinyl acetate (VAc)

Although the kinetics of vinyl acetate (VAc) free radical polymerization have not been intensively investigated, most of the kinetic parameters that are required for mapping out chain length and conversion dependent termination rate coefficient are available from the literature or accessible via additional experiments. The relevant parameters for the present studies at 80 °C are collated in Table 1.

The initial monomer concentration $c_M^0$ in bulk was calculated using the experimentally determined density at 80 °C. For the propagation rate coefficient, $k_p$, the revised PLP data obtained with a 100 Hz laser in the temperature range of 10–60 °C by Hutchinson et al. [5] were extrapolated to 80 °C. The $k_d$ value for the AIBN decomposition was determined via UV measurements with ethyl acetate as solvent, following the protocol described in Ref. [30]. For the initiation rate coefficient $k_i$, the value calculated via the activation energy and frequency factor determined via ESR measurements by Fischer et al. [26] was used. The initiator efficiency $f$ and the average termination rate coefficient $k_t$ could not be independently determined. Since $k_i$ is more than one order of magnitude lower than $k_p$, it appears that a direct measurement of $f$ via the inhibitor method [31] is not applicable to VAc. In addition to the growing macroradicals, the highly reactive inhibitor would also react directly with the initiator radical, resulting in an overestimation of $f$ determined via this method. Due to the low initiation rate, the initiator efficiency in VAc polymerization is probably slightly decreased compared to other monomers with a similar viscosity. Thus, we used a value of $f=0.5$ as a rough estimate for our calculations, conscious that this might affect the accuracy of the absolute value of our $k_t$ calculations via Eq. (3) to some extend. Further, there is no data for the average $k_t$ available in literature, e.g. determined via the single pulsed–pulsed laser polymerization (SP–PLP) method [8]. Thus, a similar average $k_t$ value of $1\times10^8$ to that of methyl acrylate [32] was used for our simulations. For the heat of polymerization literature data was employed [27], subsequently verified in several other publications [33].

Table 1
Monomer properties and kinetic parameters for vinyl acetate (VAc) at 80 °C used in the evaluation of the on-line calorimetry experiments and PREDICI® simulations

| $c_M^0$ (mol L$^{-1}$) | $k_p$ (L mol$^{-1}$ s$^{-1}$) | $k_d$ (s$^{-1}$) | $k_i$ (L mol$^{-1}$ s$^{-1}$) | $f$ | $k_t$ (L mol$^{-1}$ s$^{-1}$) | $-\Delta H$ (K J mol$^{-1}$) |
|---|---|---|---|---|---|---|
| 9.9 | 14,400 | $1.1\times10^{-4}$ | 233 | 0.5 | $1\times10^{8}$ or CLD | 88 |

The selection criteria are explained in the text.

Since a non-ideal polymerization behaviour of VAc [6] and evidence for chain transfer reactions [25] have been found, it is important to obtain the monomer reaction order experimentally under conditions similar to those used for the RAFT-CLD-T experiments.

For this purpose, calorimetric measurements of the heat of polymerization at 80 °C, using AIBN as initiator and ethyl acetate as solvent (which is electronically and sterically very similar to VAc) were carried out. Since we are mapping the rate of polymerization, $R_p$, as a function of time up to high conversions, the entire $R_p(t)$ trace of a bulk and three diluted samples can be employed to deduce the reaction order. The advantage of this procedure is that the influence of the polymer concentration on the rate of polymerization can also be determined. However, it must be considered in the calculations that the initiator concentration decreases with increasing reaction time. It was previously shown that the monomer reaction order, $\omega$, can be obtained via Eq. (4), whereby $c$ is the proportionally constant [19].

$$\log(R_p) - \log[I]^{0.5} - \log(c) = \omega \log[M] \quad (4)$$

The rate of polymerization can also be used to calculate the actual (current) monomer concentration via Eq. (5).

$$[M] = [M]_0 - \int_0^t R_p(t)\mathrm{d}t \quad (5)$$

Since the absolute value of $c$ in Eq. (4) is insignificant for the slope, $\omega$, the only parameters required with high accuracy are $\Delta H$ and $k_d$ (Table 1). Fig. 1 depicts an analysis of the $R_p(t)$ data via Eq. (4) at 80 °C (Fig. 1).

Inspection of Fig. 1 indicates that for all monomer concentrations a rapid increase of the rate is observed until the steady state is attained (right hand side of each curve). After reaching steady state conditions, the rate in the bulk sample increases due to a strong and very early Trommsdorff effect until it subsequently decreases with decreasing monomer concentration. In the diluted samples, the rate decreases immediately after reaching steady state conditions. The full line, which was constructed by fitting the zero conversion values of all curves, was used to deduce the monomer reaction order via its slope ($\omega = 1.17 \pm 0.05$). Since the full line represents the rate of polymerization without polymer content, the deviations in all samples to higher rates are a result of the gel effect, depending on the polymer content of each sample.

With $\omega = 1.17$, the magnitude of the apparent monomer reaction order of VAc is much lower than whose found for acrylates ($\omega = 1.75$ for methyl acrylate [23] and dodecyl acrylate [19]), in which chain transfer reactions are the major reason for the unexpected increase. Although evidence for chain transfer in VAc polymerization (at a lesser extend compared to acrylates) could be found [25], such reactions cannot a priori be assigned as reason for the relatively low deviation in $\omega$ from unity. Since the preferred chain transfer reaction is towards the methyl side-group, the primary radical formed may be reactive enough to add monomer at a rate similar to the end-chain radical, thus causing no significant rate retardation and effects in the monomer reaction order. It is also possible that the major contribution to the observed apparent reaction order comes from chain length dependent termination [34]. In this case, the use of a RAFT/MADIX agent would switch off the apparent effect and any consideration of a higher monomer reaction order than unity by application of the RAFT-CLD-T method would worsen the result.

To demonstrate the impact of a chain length dependent termination rate on the apparent monomer reaction order, kinetic simulations using the program package PREDICI® and steps I, IIIa, Va, Vb and Vd in the kinetic scheme depicted in Scheme 2 were carried out. The kinetic data used for the simulation are listed in Table 1. In order to allow for a direct comparison with the experimental data, the same initiator

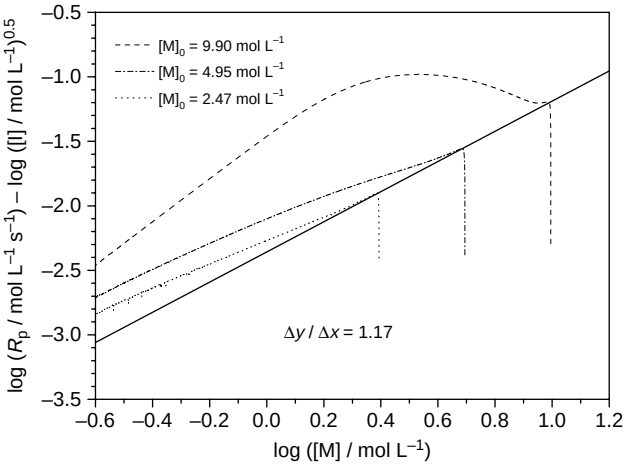


Fig. 1. Determination of the monomer reaction order, $\omega$, in vinyl acetate (VAc) free radical polymerizations at 80 °C. The plot depicts the evolution of $\log(R_p(t)) - \log[I]^{0.5}$ over the entire conversion range for the bulk and solution polymerizations (with ethyl acetate as solvent). The data were obtained by measuring the heat of polymerization and calculating the corresponding rate using literature values for $\Delta H$. The initial monomer concentrations are given within the figure. The AIBN concentration was $3.2\times10^{-3}$ mol L$^{-1}$ in each case. The full line was constructed by fitting the initial part of the plots (see text for details) for all concentrations. The slope for the fit represents the reaction order.

concentration of $3.22\times10^{-3}$ mol $L^{-1}$ was used and the results are plotted analogous to Fig. 1. In the first case, a constant $k_t$ of $1\times10^8$ L $mol^{-1}$ $s^{-1}$ was employed, in the second case a chain length dependent termination rate coefficient $k_t^{i,i}$ was used. The chain length dependence was implemented using the frequently used power law (Eq. (6)) [35] and an $\alpha$ value of 0.16, which was theoretically predicted for the long chain length regime by Friedman and O'Shaughnessy [36].

$$k_t^{i,i} = k_t^0 i^{-\alpha} \tag{6}$$

$k_t^0$ was selected to yield a $k_t^{i,i}$ value of $1\times10^8$ L $mol^{-1}$ $s^{-1}$ at a number average molecular weight $M_n = 1\times10^6$. To meet this condition, $k_t^0$ must be set to $4.47\times10^8$ L $mol^{-1}$ $s^{-1}$. The resulting simulated apparent monomer reaction orders alongside the corresponding macroradical molecular weights are depicted in Fig. 2(a) and (b), respectively.

Inspection of Fig. 2(a) demonstrates that already without employing a chain length dependent termination rate coefficient, the monomer reaction order determined from the slope is slightly higher than unity. This is a result of the increased portion of recombination of initiator fragments with ongoing monomer to polymer conversion, which would correspond to a decrease of the initiator efficiency with conversion. Using a chain length dependent termination rate coefficient with an $\alpha$ value of 0.16, a higher monomer reaction order of $\omega = 1.10$ is returned. Fig. 2(b) depicts the $M_n$ values reaching $2.2\times10^6$ in the initial period and decreasing in an almost liner fashion up to 100% conversion. Although the impact of the kinetic chain length on conversion is strong, the apparent effect on the monomer reaction order is limited. However, with a higher value of $\alpha$, the experimental monomer reaction order of 1.17 can be obtained without consideration of transfer reactions.

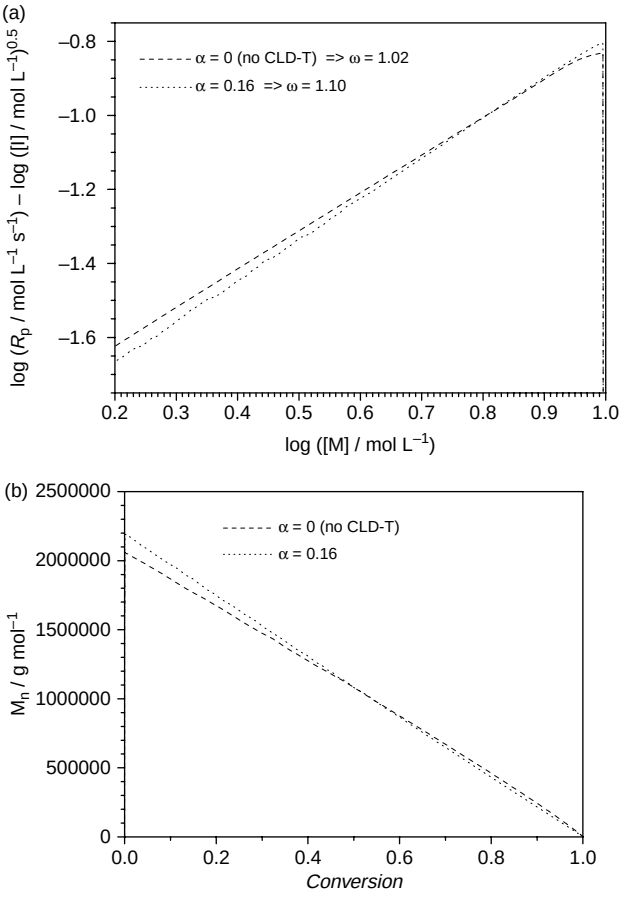


Fig. 2. (a) Simulated monomer reaction orders, $\omega$, in vinyl acetate (VAc) free radical polymerizations at 80 °C, using the PREDICI® program package and kinetic data listed in Table 1. The AIBN concentration was selected identical to the experiments (Fig. 1). The slope for the fit represents the reaction order. In (b), the corresponding number average molecular weights, $M_n$ vs. monomer to polymer conversion are depicted. The dashed lines in each figure represent the simulation results for a constant $k_t$ of $1\times10^8$ L $mol^{-1}$ $s^{-1}$. The dotted lines represent a chain length dependent termination rate coefficient with an $\alpha$ value of 0.16.

From this result, it can be concluded that the small deviation in the monomer reaction order from unity in VAc free radical polymerization is probably—at least to a large degree—a result of the chain length dependent termination rate coefficient in connection with the kinetic chain length. It is thus not advisable to employ the determined monomer reaction order in a RAFT system. Because the deviation from unity is relatively small, major effects on the result of the RAFT-CLD-T method can be ruled out, even if transfer reactions produce an abated contribution.

### 3.2. RAFT/MADIX polymerization of vinyl acetate

As mentioned in the introduction, RAFT agents with a low radical stabilization capability must be used for the polymerization of vinyl acetate, since the propagating radicals are highly reactive. Further, in context of the RAFT-CLD-T method, the fragmentation of the intermediate radicals must be fast enough to ensure that no rate retardation is induced by the RAFT process itself. In general, besides dithiocarbamates, [37] xanthates [38] are highly favourable for VAc polymerization. The xanthate mediated RAFT polymerization has been termed MADIX (macromolecular design via interchange of xanthates) by its inventors [39,40].

A recently published investigation on the influence of the RAFT/MADIX agent structure on the polymerization behaviour of vinyl acetate gives evidence that an ethoxy Z-group causes the lowest rate retardation [41] and is thus a promising function for application of the RAFT(MADIX)-CLD-T method. The R-group of the MADIX agent should be selected to be a good leaving group and should show a similar reactivity towards the addition of monomer as the growing macroradical. In general, the selection of a macroradical analogous leaving group with a chain length of unity is favourable, since its reinitiation reactivity is optimal and the fragmentation reaction probability to both sides in the pre-equilibrium (Scheme 2) is similar [18]. However, in an idealized RAFT mechanism, the fragmentation would always be directed to the opposite side to the addition, thus doubling the efficiency of the addition reaction and minimizing initial high molecular weight polymers being formed. In the pre-equilibrium, fragmentation to the opposite addition direction can be achieved by selecting an R-group with a better radical stabilization ability.

Relative information about the radical reactivities can be obtained by copolymerization of monomers. A moderately better stabilized radical is derived from a methyl acrylate (MA) macroradical. Using the reactivity ratios for the system VAc–MA, the reactivities can directly be compared. A previous $^1$H NMR spectroscopic investigation of the copolymer compositions resulted in reactivity ratios $r_{VAc}=0.04$ and $r_{MA}=7.28$ [42] by the Kelen–Tüdős method, which clearly indicates the better radical stabilization capability of MA compared to VAc. Thus, a methoxycarbonyl ethyl (MCE) R-group appears to be a better leaving group than a vinyl acetate analogous one. The general definition of the reactivity ratios is given by Eq. (7).

$$r_1 = \frac{k_{11}}{k_{12}} \tag{7}$$

With $r_1$ being the reactivity ratio of MA, $k_{11}$ is the propagation rate coefficient of MA (47,400 L mol$^{-1}$ s$^{-1}$ at 80 °C) [43], and $k_{12}$ the addition rate of VAc to the MA polymer chain end, the addition rate of the VAc monomer to the MCE leaving group can be estimated. Solving Eq. (7) for $k_{12}$ results in $k_{12}=6500$ L mol$^{-1}$ s$^{-1}$, which is approximately half of the value of $k_p$ for vinyl acetate (14,400 L mol$^{-1}$ s$^{-1}$) [5]. In the subsequent chapter we will demonstrate by modeling studies, how a decreased reinitiation rate can affect the evolution of chain length dependent termination rate coefficients by the RAFT-CLD-T method. The accordingly used 2-ethoxythiocarbonylsulfanyl-propionic acid methyl ester (EPAME) MADIX agent is depicted alongside the VAc monomer in Scheme 1.

The use of RAFT/MADIX agents with less radical stabilizing Z-groups can lead to high molecular weight polymers being formed already in the initial period [18]. It is thus necessary to prepare $M_n$ vs. conversion plots, which can be used as calibration for the chain length axis for the mapping of the termination rate coefficient chain length $i$. Fig. 3 depicts the evolution of the number average molecular weight, $M_n$, with monomer to polymer conversion for the EPAME mediated processes.

In Fig. 3 hybrid behaviour causing high molecular weight polymers being formed already in the initial period [44] is evident at all EPAME concentrations. The molecular weight evolution further shows some deviation from a linear rise—in particular for the lowest RAFT agent concentration—which was taken into account in the fitting process.

It was previously shown that the RAFT addition rate coefficient, $k_\beta$, can be estimated, as long as hybrid behaviour

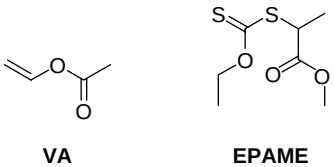


Scheme 1. Monomer vinyl acetate (VAc) and the RAFT/MADIX agent 2-ethoxythiocarbonylsulfanyl-propionic acid methyl ester (EPAME) employed in the current study.

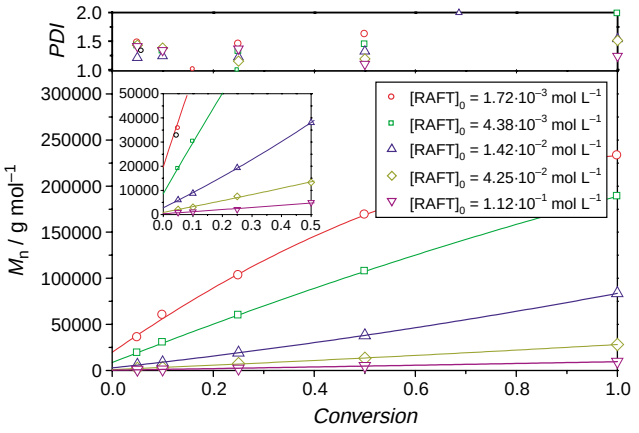


Fig. 3. Number average molecular weight, $M_n$ vs. monomer to polymer conversion in EPAME mediated bulk free radical polymerization of vinyl acetate (VAc) at 80 °C. The associated initial RAFT reagent concentrations are given within the figure. The AIBN concentration was $3.2\times10^{-3}$ mol L$^{-1}$. The curves represent a best fit for molecular weight vs. time evolutions. The $y$-axis intercepts of the best fits indicate the initial molecular weight (see Table 2 for the chain lengths). The upper part of the figure gives the corresponding polydispersity indices (PDI).

occurs (Eq. (8), see Ref. [18] for the derivation).

$$k_\beta = \frac{k_p[M]_0}{(DP_n^{inst}-1)[RAFT]_0\phi} \tag{8}$$

In Eq. (8), $DP_n^{inst}$ is the degree of the instantaneously generated polymeric material, which can be determined by extrapolation of the measured molecular weights to zero conversion. $\phi$ is the fragmentation coefficient, which gives the probability of the macroRAFT radical undergoing transfer instead of fragmenting back to the starting materials. In the case of EPAME, a fragmentation to the MCE R-group is preferred indicating a fragmentation coefficient close to unity, however there is no reliable exact information available. Further, with extrapolating $DP_n^{inst}$ from higher molecular weights, not only $k_\beta$ from the pre-equilibrium but also from the main equilibrium (where the fragmentation coefficient is 0.5) is considered. Thus, the effective fragmentation coefficient must lie somewhere between 0.5 and 1. With the experimental RAFT agent concentrations and $DP_n^{inst}$ values from Table 2 and the monomer concentrations and propagation rate coefficient of VAc at 80 °C from Table 1, the resulting $k_\beta$ calculated using an average fragmentation coefficient of $\phi=0.75$ are listed in Table 2.

For the two highest RAFT agent concentrations, the accuracy is strongly limited, since the $DP_n^{inst}$ values are very low. Thus, only the results for the three lowest RAFT agent concentrations were considered to yield the average value of $k_\beta=4.5\times10^5$ L mol$^{-1}$ s$^{-1}$. It should be noted that the accuracy of this value is further limited by the experimental scatter of the $M_n$ vs. conversion data resulting in an uncertainty in $DP_n^{inst}$, the overall error is therefore estimated to be $2\times10^5$ L mol$^{-1}$ s$^{-1}$.

To demonstrate the effect of the calculated $k_\beta=4.5\times10^5$ L mol$^{-1}$ s$^{-1}$ and impact of the fragmentation rate coefficient on the shape of the $M_n$ vs. conversion plots,

Table 2
Summary of the initial EPAME concentrations in vinyl acetate (VAc) bulk polymerizations as well as the associated degrees of polymerization of the instantaneously generated polymer, $DP_n^{inst}$, at 80 °C

| $c^0_{RAFT}$ (mol $L^{-1}$) | $DP_n^{inst}$ | $k_\beta$ (L $mol^{-1}$ $s^{-1}$) |
|---|---|---|
| $1.72\times10^{-3}$ | 229 | $4.8\times10^5$ |
| $4.38\times10^{-3}$ | 100 | $4.4\times10^5$ |
| $1.42\times10^{-2}$ | 32 | $4.3\times10^5$ |
| $4.25\times10^{-2}$ | 10 | $(5.0\times10^5)$ |
| $1.12\times10^{-1}$ | 3 | $(7.9\times10^5)$ |

The initiator concentration (AIBN) was close to $3.2\times10^{-3}$ mol $L^{-1}$. The $k_\beta$ values that have been deduced via Eq. (8) are included as well (for details see text and the associated Fig. 3).

PREDICI® simulations via the kinetic scheme given in Scheme 2 were carried out. For this purpose, the kinetic data from Table 1, the experimental MADIX agent concentrations, and the average $k_\beta$ value, as well as an $k_{-\beta}$ value of $1\times10^4$ $s^{-1}$ were used.

For the pre-equilibrium, the limiting cases of an equal fragmentation to both sides ($k_{\beta,1}=k_{\beta,2}=k_\beta$ and $k_{-\beta,1}=k_{-\beta,2}=k_{-\beta}$) and an exclusive fragmentation towards the MCE R-group ($k_{-\beta,1}$ and $k_{\beta,2}=0$) were considered. The resulting simulated $M_n$ vs. conversion plots are depicted in Fig. 4.

Fig. 4 clearly shows the effect of a good leaving group, halving the simulated $DP_n^{inst}$ values, which are given by the dashed lines. It is further remarkable that the deviations in the $M_n$ vs. conversion plots from the linear behaviour as well as the polydispersities are very similar to those observed experimentally (Fig. 3). In both cases the molecular weights for the lowest RAFT agents concentration show a deviation to lower values at high conversions, which is a result of high amounts of initiated and terminated polymer chains compared to the overall number of living chains given by the initial RAFT agent concentration. This also results in a rise of the polydispersity, which can be clearly observed in the simulated and experimental data. Differences in the exact shape between the simulated and experimental plots are probably due to the chain length dependence of the termination rate coefficient, which was not considered in the simulations.

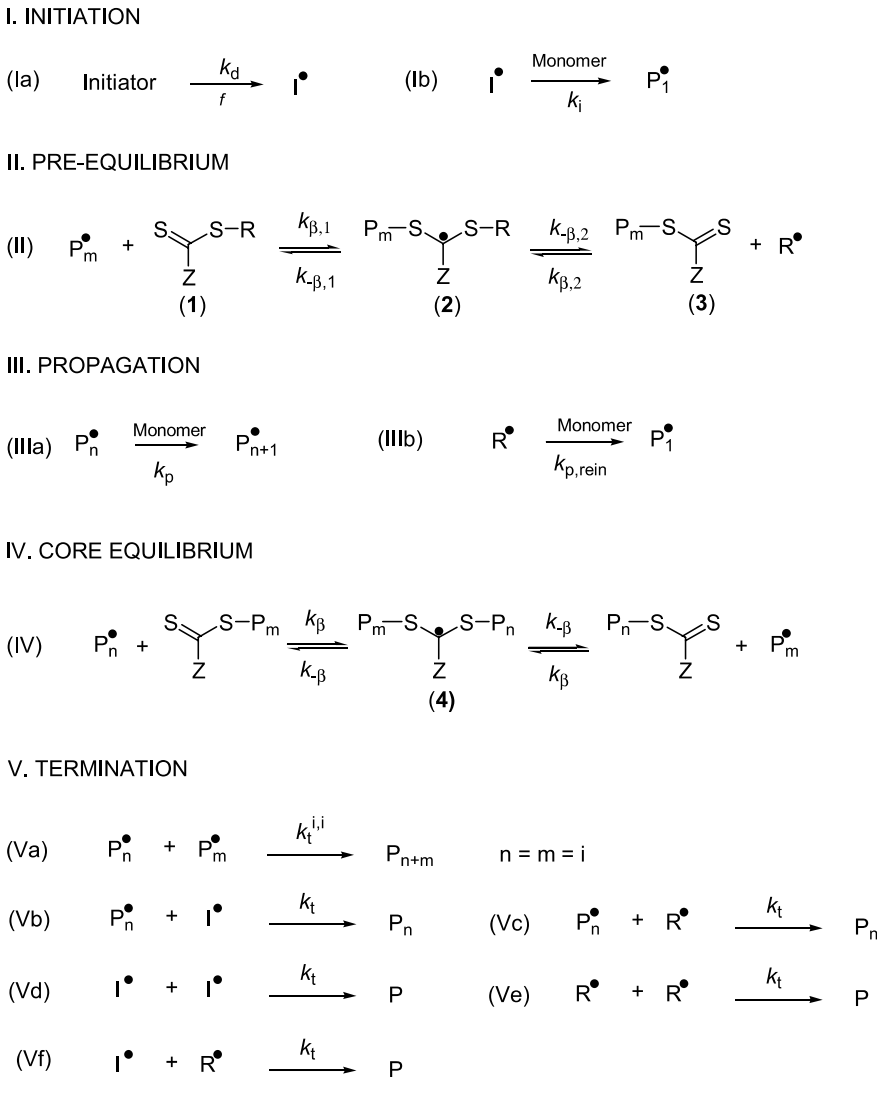


Scheme 2. Reaction sequence used for the kinetic simulations of the RAFT process via the PREDICI® program package.

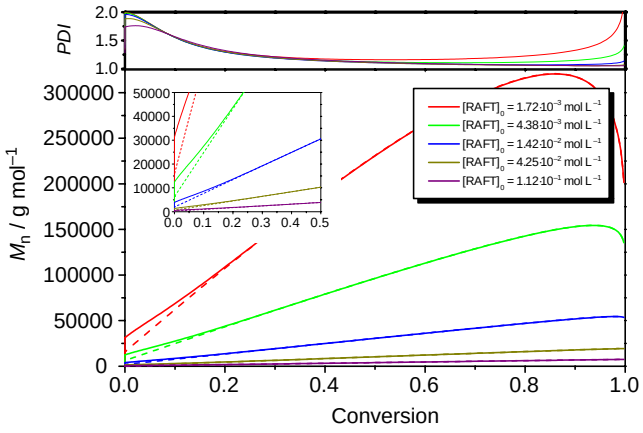


Fig. 4. Simulated number average molecular weight, $M_n$ vs. monomer to polymer conversion in EPAME mediated bulk free radical polymerization of vinyl acetate (VAc) at 80 °C, using the PREDICI® program package and kinetic data listed in Table 1. The initial RAFT reagent and AIBN concentrations were selected identical to the experiments (Fig. 3). The full lines represent an equal fragmentation to both sides, the dashed lines an exclusive fragmentation towards the MCE R-group. The upper part of the figure gives the polydispersity indices (PDI), in case of an exclusive fragmentation towards the MCE R-group.

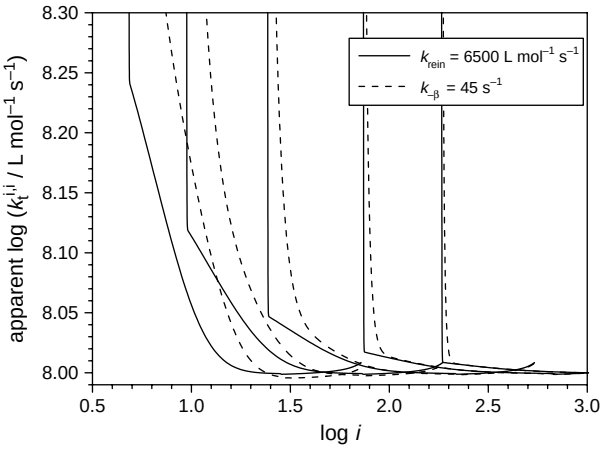


Fig. 5. Simulated apparent experimental termination rate coefficient for vinyl acetate (VAc) radical polymerization at 80 °C using the PREDICI® program package, the kinetic data listed in Table 1, and the experimental initiator and RAFT agent concentrations (Fig. 3). For $k_\beta$, the average value of the results listed in Table 2 ($4.5\times10^5$ L mol$^{-1}$ s$^{-1}$) was used. The full line is constructed using a $k_{-\beta}$, of $1\times10^4$ s$^{-1}$, and $k_{rein}$ as calculated from Eq. (7) (6500 L mol$^{-1}$ s$^{-1}$), see text for details. The dashed line represents a slow fragmentation of the RAFT intermediate radicals ($k_{-\beta}$=45 s$^{-1}$). To avoid an overlap of several effects, $k_{rein}$ was selected identical to the propagation rate coefficient in this simulation (14,400 L mol$^{-1}$ s$^{-1}$).

### 3.3. Chain length and conversion dependent termination rate coefficients

In a previous article [23], we have exemplified the mapping of chain length and conversion dependent termination rate coefficients, using methyl acrylate (MA) as monomer and methoxycarbonylethyl phenyldithioacetate (MCEPDA) as RAFT agent. From a closer inspection of Fig. 1, it becomes evident that VAc shows a similarly strong and early gel effect as MA, indicating that $k_t$ of VAc is similarly strongly conversion dependent. In order to cover both effects—the chain length and conversion dependence—of $k_t$ in VAc polymerization, it is highly favourable to use the same method for the data evaluation as in Ref. [23].

In addition to the experiments described in the previous chapters, it must be excluded that a low initiation rate coefficient, $k_i$, (Table 1), a low fragmentation rate in the RAFT equilibrium, and a low reinitiation rate of the leaving R-group affects the results. The influence of such effects can easily be accessed by modeling studies, using the PREDICI® program package and the kinetic scheme depicted in Scheme 2. Similar to the studies described in Ref. [18], we implemented a slightly simplified variation of Eq. (3) without consideration of the differential non-steady state term into PREDICI® and calculated the apparent log($k_t^{i,i}$) vs. log($i$) graphs for different scenarios. The kinetic parameters from Table 1 were used for the simulations. For the ease of comparison, $k_t$ was selected to be chain length independent. The addition rate coefficient of the macroradical to the RAFT agent, $k_\beta$, was set to an average value of $4.5\times10^5$ L mol$^{-1}$ s$^{-1}$, using the data from Table 2. In all simulations a small $k_i$ was employed. The effects of a reduced $k_{rein}$ of 6500 L mol$^{-1}$ s$^{-1}$ as estimated in the previous chapter and a slow fragmentation of the RAFT intermediate radicals, $k_{-\beta}$, were probed separately. To ensure a fast fragmentation in the first case, a $k_{-\beta}$ of $1\times10^4$ L mol$^{-1}$ s$^{-1}$ was selected. The results of the simulations using the experimental initiator and RAFT agent concentrations are depicted in Fig. 5.

The full lines in Fig. 5 represent an ideal RAFT equilibrium, in which steady state conditions are reached fast (almost vertical line on the left hand side). However, before reaching the default value of 8 in log($k_t^{i,i}$), the reduced reinitiation rate induces an apparently higher termination rate coefficient and a chain length dependent behaviour, although $k_t$ was set to a constant value. The magnitude of this effect is dependent on the RAFT agent concentration, reaching a maximum of 0.24 logarithmic units for the highest RAFT agent concentration. At the end of each curve, the apparent $k_t^{i,i}$ rises again about 0.01 logarithmic units at 80% conversion because of the low $k_i$ value, which induces primary radical termination and self-termination of the AIBN derived radicals at low monomer concentrations. Although the difference between $k_i$ and $k_p$ in VAc polymerization is much more pronounced than in acrylate systems, the effect on the $k_t$ data is still minimal and can be neglected. The dashed lines in Fig. 5 represent a slow fragmentation of the RAFT intermediate radicals, which considerably increases the time to reach steady state radical concentration and also induces apparently higher $k_t^{i,i}$ values and a chain length dependent behaviour. These results are fully consistent with earlier modeling studies, which were carried out in the conversion vs. time domain [45].

In contrast to a low $k_{-\beta}$ value (which may be operative in some RAFT agent/monomer systems) the reduced $k_{rein}$ can be expected in the current system (see previous chapter). It is thus important to assess how a lower $k_{rein}$ value (compared to the

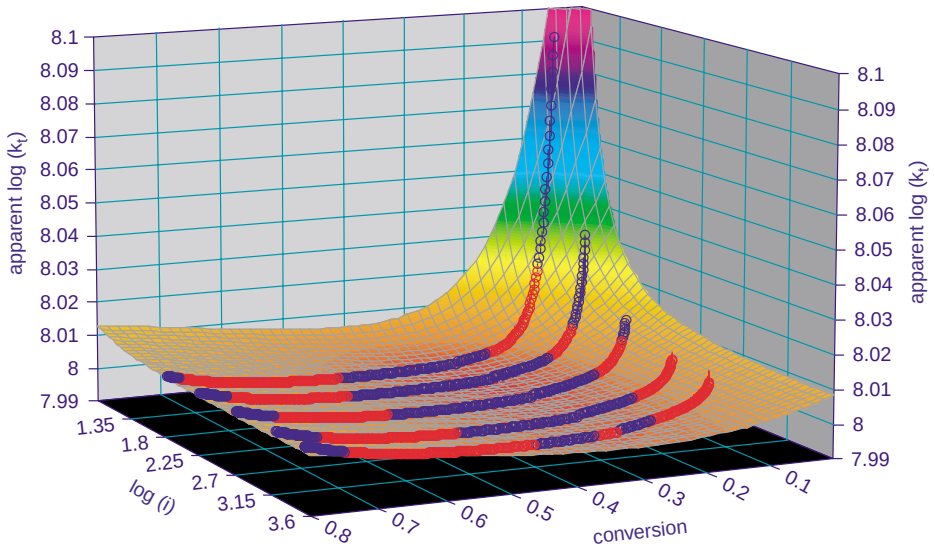


Fig. 6. Three-dimensional plot of the simulated apparent termination rate coefficient for vinyl acetate (VAc) radical polymerization at 80 °C using the PREDICI® program package, the kinetic data listed in Table 1, and the experimental initiator and RAFT agent concentrations (Fig. 3). For $k_{\beta}$, the average value of the results listed in Table 2 ($4.5\times10^{5}$ L mol$^{-1}$ s$^{-1}$) was used, for $k_{-\beta}$, an value of $1\times10^{4}$ s$^{-1}$ was selected, which does not cause any rate retardation effects. $k_{rein}$ was selected as calculated from Eq. (7) (6500 L mol$^{-1}$ s$^{-1}$), see text for details. The $k_t$ values are plotted vs. monomer conversion and chain length and are fitted to a surface plot using the TableCurve® 3D software. The units for the apparent termination rate coefficient are L mol$^{-1}$ s$^{-1}$.

magnitude of the propagation rate coefficient) can influence the data evaluation procedure. Fig. 6 depicts the simulated apparent log($k_t$) values plotted vs. the monomer to polymer conversion and chain length axis in a three dimensional plot, using the estimated $k_{rein}$ value of 6500 L mol$^{-1}$ s$^{-1}$. The conversion range covered in this simulation starts at 5% and reaches up to 80%, which are realistic limits for the experimental data evaluation.

It can clearly be seen from Fig. 6 that the reduced $k_{rein}$ value results in an increased apparent log($k_t$) value in the small conversion–small chain length area. To prevent that this effect superimposes the experimental data from the RAFT-CLD-T method, the affected data must be removed. For this purpose, a maximum log($k_t$) value of 8.01 in the simulated data was set as a confidence limit for the experimental data. For the highest RAFT agent concentration of $1.12\times10^{-1}$ mol L$^{-1}$, this limit was reached at 12.5% conversion, the lower RAFT agent concentration of $4.25\times10^{-2}$ mol L$^{-1}$ allows for a reliable data evaluation starting at 9% monomer to polymer conversion, and the intermediate RAFT agent concentration of $1.42\times10^{-2}$ mol L$^{-1}$ above 5.5%. The lower RAFT agent concentrations are not affected above 5% conversion.

Using those conversion ranges, the experimental time dependent $k_t$ data calculated via Eq. (3) were plotted vs. the monomer to polymer conversion and chain length axis (calibrated by the experimentally determined $M_n$ vs. conversion functions from Fig. 3) in a three-dimensional plot (Fig. 7).

Inspection of Fig. 7 does not show any major deviation of log($k_t$) in the small conversion–small chain length area, indicating that no significant effects caused by a slow fragmentation of the RAFT intermediate radicals (Fig. 5) or a remainder of the effect caused by a slow reinitiation are present. However, it should be noted that the absolute level of the extracted $k_t$ values might be beset with an error of $\pm0.3$ logarithmic units, since the initiator efficiency, $f$, could not be determined and the propagation rate coefficient, $k_p$, was extrapolated from measured data in the temperature range of 10–60 °C. The data were fitted to a surface graph, using TableCurve® 3D as fitting software. The obtained surface function involves several calculation steps and can be found in form of a BASIC file in the supporting information section. The function input parameters are the conversion and the logarithmic chain length, where the conversion range can be between 0.05 and 0.8 and the logarithmic chain length between 1.25 and 3.25. Thus, specific values for $k_t(X, i)$ can be calculated.

For a more detailed analysis of the result, slash graphs over the conversion range for different chain lengths (Fig. 8) were prepared.

Fig. 8 clearly indicates that $k_t$ decreases with an increasing chain length (log($i$) from 1.25 to 3.25). For all chain lengths, the log($k_t$) vs. log($i$) functions curve downwards, which is very similar to the plateau areas found at low conversions for MA polymerization, followed by a stronger decrease of $k_t$ at higher conversions [23,46]. In general, it should be noted that the $k_t(X)$ functionality is influenced by the initiator efficiency, which was assumed to decrease linearly with conversion. Such an assumption seems to be justified, since linear or quasi-linear functionalities have been previously reported (see for example Ref. [47]). Since the functionality of $f$ is linear in the enumerator in Eq. (1), any possible minor deviation from the proposed conversion dependency of $f$ would be directly proportional to $k_t$, however inducing only limited changes in log ($k_t$). In contrast to the data presented here, $k_t$ values determined by different methods are averaged over several chain lengths ($i$ up to 5000) and thus represent an average of $k_t$

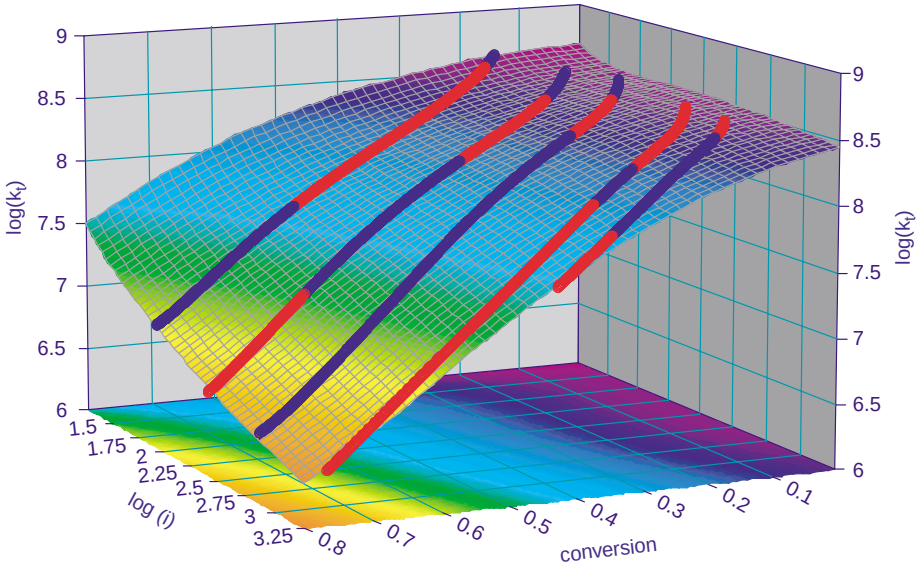


Fig. 7. Three-dimensional plot of the termination rate coefficient for vinyl acetate (VAc) radical polymerization at 80 °C, employing five initial RAFT agent concentrations ($1.72\times10^{-3}$, $4.38\times10^{-3}$, $1.42\times10^{-2}$, $4.25\times10^{-2}$ and $1.12\times10^{-1}$ mol $L^{-1}$). The AIBN concentration was close to $3.2\times10^{-3}$ mol $L^{-1}$. The $k_t$ values are plotted vs. monomer conversion and chain length and are fitted to a surface plot using the TableCurve® 3D software. The correlation coefficient of the fit is $r^2>0.9993$ with the red and blue parts of the experimental data indicating very minor under- and overestimates of the fitted surface. The units for the termination rate coefficient are L $mol^{-1}$ $s^{-1}$.

at all covered chain lengths. The dotted line in Fig. 8, representing the conversion dependence of $k_t$ for $i=1778$, has a similar functionality as the conversion dependence of $k_t$ for $i=1000$ in MA polymerization [23]. For shorter chain lengths, the conversion dependence of $k_t$ is less pronounced, as can be expected from theory, since the increase of viscosity and the size of the moving polymer chains are reduced.

Fig. 9 illustrates the evolution of $\log(k_t)$ over the chain length for different conversions.

Because of hybrid behaviour and the removed data due to slow reinitiation, chain lengths below 18 ($\log(i)=1.25$) could not be covered. For the examined chain length regime up to 1778 ($\log(i)=3.25$), a relatively small chain length dependence could be observed at low monomer to polymer conversion, which is close to a linear behaviour. At higher conversions, the decrease of $k_t$ with increasing chain lengths becomes more pronounced, in particular at the smaller chain lengths region, which may be attributed to the region at which intermolecular entanglements build up. Since the chain length dependence in general is linear with some sporadic deviations, the graphs were fitted via the frequently used expression $k_t^{i,i}=k_t^0 i^{-\alpha}$ [35]. The resulting $\alpha$ values are listed in Table 3. Since our data evaluation method is very stable with regard to the extraction of $\alpha$ values [20], we believe that the absolute error in $\alpha$ is below 0.05.

The data entries in Table 3 show a similar trend with strongly increasing $\alpha$ values towards higher conversion as observed in MA polymerizations [23], underpinning the notion that $\alpha$ is a function of monomer to polymer conversion. However, in general the values for VAc are significantly

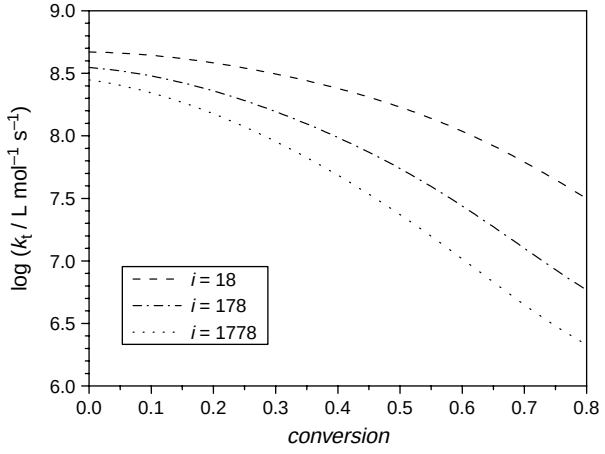


Fig. 8. Extracted $k_t$ vs. conversion data from Fig. 7 for three different chain lengths.

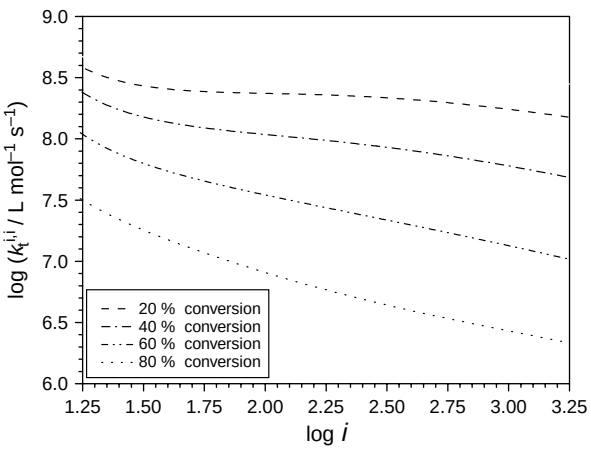


Fig. 9. Extracted $k_t$ vs. chain length data from Fig. 7 for four different conversions.

Table 3
$\alpha$ Values (in the equation $k_t^{i,i} = k_t^0 i^{-\alpha}$) obtained for different conversions (Fig. 9)

| Conversion (%) | $\alpha$ |
|---|---|
| 10 | 0.09 |
| 20 | 0.14 |
| 30 | 0.20 |
| 40 | 0.28 |
| 50 | 0.37 |
| 60 | 0.46 |
| 70 | 0.53 |
| 80 | 0.55 |

smaller. This may be—at least in parts—a result of the reduced amount of midchain radicals in VAc polymerization, eliminating the stronger chain length effects in termination of non-chain end radicals [36,48].

Recently, there has been a lively discussion within the scientific community on whether the propagation rate coefficient, $k_p$, is equally beset by a chain length dependence [49]. A potential chain length dependence of $k_p$ may alter the outcome of the above analysis procedures for small chain lengths [50]. Many techniques (including SP–PLP and RAFT-SP–PLP) are affected by CLD $k_p$ data to some extend. Whilst there is some agreement that $k_p$ is in all likelihood chain length dependent, there is significant disagreement to what extend. Most studies regarding the chain length have been carried out for styrene and methyl methacrylate (MMA), with no report on VAc. The most significant decrease in $k_p$ with chain length should occur at small $i$ (i.e. when going from 1 to 5 units). However, the critical region ($i<18$) is omitted in our three dimensional analysis and also in the data given in Fig. 9. In addition, every conceivable chain length dependency of $k_p$ can be evaluated with our present data with relative ease, resulting in modified $\log(k_t)$ functions in the oligomeric region.

## 4. Conclusions

In the present contribution we have applied living free radical polymerization technology (MADIX) to gain accesses to chain length and conversion dependent termination rate coefficients of vinyl acetate (VAc). PREDICI® simulations were employed to probe potential non-ideal free radical polymerization kinetics of VAc (monomer reaction orders different from unity) and rate retardation phenomena due to application of the RAFT/MADIX agent. As a result, the RAFT(MADIX)-CLD-T methodology can be applied with a monomer reaction order of unity, since VAc displays a significantely lower monomer reaction order than arcylates ($\omega$(VAc, 80 °C)=1.17 vs. $\omega$(MA, DA, 80 °C)=1.75). The small deviation from unity of the mononer reaction order may be understood in terms of chain length dependent termination. The increase in reaction order when going from VAc to the acrylates is likely associated with an increased presence of midchain radicals. The $\alpha$ value (in the often employed expression $k_t(i,i) = k_t^0 i^{-\alpha}$) reads 0.09 at low conversion (10%) and increases significantely towards larger conversions ($\alpha=0.55$ at 80%). Due to hybrid behaviour and a relatively slow reiniation of the leaving R-group of the RAFT agent with VAc ($k_{rein}=6500\ L\ mol^{-1}\ s^{-1}$), $k_t(i,i)$ cannot be mapped for very low chain lengths. The RAFT-CLD-T technique also allowed for mapping of $k_t$ as a function of conversion at constant chain lengths. Similar to observations made earlier in acrylate systems, the decrease of $k_t$ with conversion is more pronounced at increased chain lengths.

## Acknowledgements

We are grateful for financial support from the Australian Research Council (ARC) in the form of a Discovery Grant (to C.B.-K. and M.H.S.). T.P.D. acknowledges an Australian Federation Fellowship (ARC). We thank Dr Luca Albertin for the provision of the employed MADIX agent as well as Dr Leonie Barner and Mr Istvan Jacenyik for their excellent management of CAMD.

## Supplementary data

Supplementary data associated with this article can be found, in the online version, at 10.1016/j.polymer.2005.12.054

## References

[1] Kost J. Controlled drug delivery systems. Polymeric materials encyclopedia. Boca Ration, FL: CRC Press; 1996 p. 1509.
[2] Hassan CM, Peppas NA. Adv Polym Sci 2000;153:37–65.
[3] Lee KY, Mooney DJ. Chem Rev 2001;101(7):1869–80.
[4] Hutchinson RA, Richards JR, Aronson MT. Macromolecules 1994; 27(16):4530–7.
[5] Hutchinson RA, Paquet Jr DA, McMinn JH, Beuermann S, Fuller RE, Jackson C. DECHEMA Monographs 1995;131:467–92.
[6] McKenna TF, Villanueva A. J Polym Sci, Polym Chem 1999;37(5): 589–601.
[7] Jovanović R, Dubé MA. J Appl Polym Sci 2004;94(3):871–6.
[8] Barner-Kowollik C, Buback M, Egerov M, Fukuda T, Goto A, Olaj OF, et al. Prog Polym Sci 2005;30(6):605–43.
[9] (a) Olaj OF, Vana P. Macromol Rapid Commun 1998;19(8):433–9.
(b) Olaj OF, Vana P. Macromol Rapid Commun 1998;19(10):533–8.
[10] de Kock JBL, Klumperman B, van Herk AM, German AL. Macromolecules 1997;30(22):6743–53.
[11] Buback M, Busch M, Kowollik C. Macromol Theory Simul 2000;9(8): 442–52.
[12] Buback M, Egorov M, Feldermann A. Macromolecules 2004;37(5): 1768–76.
[13] Buback M, Egorov M, Junkers T, Panchenko E. Macromol Rapid Commun 2004;25(10):1004–9.
[14] Buback M, Egorov M, Junkers T, Panchenko E. Macromol Chem Phys 2005;206(3):333–41.
[15] Vana P, Davis TP, Barner-Kowollik C. Macromol Rapid Commun 2002; 23(16):952–6.
[16] (a) Mayadunne RTA, Rizzardo E, Chiefari J, Chong YK, Moad G, Thang SH. Macromolecules 1999;32(21):6977–80.
(b) Moad G, Chiefari J, Chong YK, Krstina J, Mayadunne RTA, Postma A, et al. Polym Int 2000;49(9):993–1001.
(c) Chong YK, Le TPT, Moad G, Rizzardo E, Thang SH. Macromolecules 1999;32(6):2071–4.

(d) Barner-Kowollik C, Davis TP, Heuts JPA, Stenzel MH, Vana P, Whittaker M. J Polym Sci, Polym Chem 2003;41(3):365–75.
(e) Destarac M, Charmot D, Franck X, Zard SZ. Macromol Rapid Commun 2000;21(15):1035–9.
(f) Moad G, Rizzardo E, Thang SH. Aust J Chem 2005;58(6):379–410.
[17] Feldermann A, Stenzel MH, Davis TP, Vana P, Barner-Kowollik C. Macromolecules 2004;37(7):2404–10.
[18] Theis A, Feldermann A, Charton N, Stenzel MH, Davis TP, Barner-Kowollik C. Macromolecules 2005;38(7):2595–605.
[19] Theis A, Feldermann A, Charton N, Davis TP, Stenzel MH, Barner-Kowollik C. Polymer 2005;46(18):6797–809.
[20] Junkers T, Theis A, Buback M, Davis TP, Stenzel MH, Vana P, Barner-Kowollik C. Macromolecules 2005;38(23):9497–508.
[21] Johnston-Hall G, Theis A, Monteiro M, Davis TP, Stenzel MH, Barner-Kowollik C. Macromol Chem Phys 2005;206(20):2047–53.
[22] Buback M, Junkers T, Vana P. Macromol Rapid Commun 2005;26(10): 796–802.
[23] Theis A, Davis TP, Stenzel MH, Barner-Kowollik C. Macromolecules 2005;38(24):10323–7.
[24] Barner-Kowollik C, Quinn JF, Nguyen TLU, Heuts JPA, Davis TP. Macromolecules 2001;34(22):7849–57.
[25] Britton D, Heatley F, Lovell PA. Macromolecules 1998;31(9):2828–37.
[26] Fischer H, Radom L. Angew Chem, Int Ed 2001;40(8):1340–71.
[27] Tong LKJ, Kenyon WO. J Am Chem Soc 1947;69(9):2245–6.
[28] Cané F, Capaccioli T. Eur Polym J 1978;14(3):185–8.
[29] Strazielle C, Benoit H, Vogl O. Eur Polym J 1978;14(5):331–4.
[30] Charton N, Feldermann A, Theis A, Davis TP, Stenzel MH, Barner-Kowollik C. J Polym Sci, Polym Chem 2004;42(20):5170–9.
[31] Fernández-Garcia M, Fernández-Sanz M, Madruga EL. Macromol Chem Phys 2000;201(14):1840–5.
[32] Buback M, Kuelpmann A, Kurz C. Macromol Chem Phys 2002;203(8): 1065–70.
[33] Leonard J. In: Brandrup J, Immergut EH, Grulke EA, editors. Polymer handbook. 4th ed. New York: Wiley; 1999. p. II/370 [literature cited therein].
[34] Russell GT. Macromol Theory Simul 1995;4(3):519–48.
[35] Barner-Kowollik C, Vana P, Davis TP. In: Matyjaszewski K, Davis TP, editors. Handbook of radical polymerization. New York: Wiley; 2002. p. 209 [literature cited therein].
[36] Friedman B, O'Shaughnessy B. Macromolecules 1993;26(21):5726–39.
[37] Destrac M, Charmot D, Franck X, Zard SZ. Macromol Rapid Commun 2000;21(15):1035–9.
[38] Rizzardo E, Chiefari J, Mayadunne RTA, Moad G, Thang SH. ACS Symp Ser 2000;768:278–96.
[39] Taton D, Wilczewska AZ, Destrac M. Macromol Rapid Commun 2001; 22(18):1497–503.
[40] Destrac M, Bzducha W, Taton D, Gauthier-Gillaizeau I, Zard SZ. Macromol Rapid Commun 2002;23(17):1049–54.
[41] Stenzel MH, Cummins L, Roberts GE, Davis TP, Vana P, Barner-Kowollik C. Macromol Chem Phys 2003;204(9):1160–8.
[42] Brar AS, Charan S. J Appl Polym Sci 1994;53(13):1813–22.
[43] Buback M, Kurz CH, Schmaltz C. Macromol Chem Phys 1998;199(8): 1721–7.
[44] Barner-Kowollik C, Quinn JF, Nguyen TLU, Heuts JPA, Davis TP. Macromolecules 2001;34(22):7849–57.
[45] Vana P, Davis TP, Barner-Kowollik C. Macromol Theoy Simul 2002; 11(8):823–35.
[46] Kowollik C. PhD Thesis. University of Göttingen, ISBN 3-89712-705-9; 1999.
[47] Buback M, Huckstein B, Kuchta FD, Russell GT, Schmidt E. Macromol Chem Phys 1994;195(6):2117–40.
[48] Buback M, Egorov M, Feldermann A. Macromolecules 2004;37(5): 1768–76.
[49] (a) Willemse RXE, Staal BBP, van Herk AM, Pierik SCJ, Klumperman B. Macromolecules 2003;36(26):9797–803.
(b) Olaj OF, Vana P, Zoder M, Kornherr A, Zifferer G. Macromol Rapid Commun 2000;21(13):913–20.
(c) Olaj OF, Vana P, Zoder M. Macromolecules 2002;35(4):1208–14.
(d) Zetterlund PB, Busfield WK, Jenkins ID. Macromolecules 2002; 35(19):7232–7.
(e) Smith GB, Russell GT, Yin M, Heuts JPA. Eur Polym J 2005;41(2): 225–30.
[50] Heuts JPA, Russell GT. Eur Polym J 2006;42(1):3–20.